Pharmacogenetic modulation of STEP improves motor and cognitive function in a mouse model of Huntington's disease

Marta Garcia-Forna [b, c, 1], Sara Martínez-Torres [a, 1, 2], Gerardo García-Díaz Barriga [a, b, c], Jordi Alberch [a, b, c], Montse Milà [b, d], Garikoitz Azkona [a, b, c], Esther Pérez-Navarroa, [b, c, *]

a Departament de Biomedicina, Facultat de Medicina i Ciències de la Salut, Institut de Neurociències, Universitat de Barcelona, Barcelona, Catalonia, Spain

b Institut d'Investigacions Biomèdiques August Pi i Sunyer (IDIBAPS), Barcelona, Catalonia, Spain

c Centro de Investigación Biomédica en Red sobre Enfermedades Neurodegenerativas (CIBERNED), Spain

d Departament de Genètica, Hospital Clínic de Barcelona, Barcelona, Catalonia, Spain

* Corresponding author at: Dept. Biomedicina, Facultat de Medicina i Ciències de la Salut, Institut de Neurociències, Universitat de Barcelona, Casanova 143, 08036 Barcelona, Catalonia, Spain.

Email address: estherperez@ub.edu (E. Pérez-Navarro)

1 These authors contributed equally to this work.

2 Present address: Laboratory of Neuropharmacology, Department of Experimental and Health Sciences, University Pompeu Fabra, Barcelona, Catalonia.

ABSTRACT

Huntington's disease (HD) is a hereditary neurodegenerative disorder caused by an expansion of a CAG repeat in the huntingtin (htt) gene, which results in an aberrant form of the protein (mhtt). This leads to motor and cognitive deficits associated with corticostriatal and hippocampal alterations. The levels of STriatal-Enriched protein tyrosine Phosphatase (STEP), a neural-specific tyrosine phosphatase that opposes the development of synaptic strengthening, are decreased in the striatum of HD patients and also in R6/1 mice, thereby contributing to the resistance to excitotoxicity described in this HD mouse model. Here, we aimed to analyze whether STEP inactivation plays a role in the pathophysiology of HD by investigating its effect on motor and cognitive impairment in the R6/1 mouse model of HD. We found that genetic deletion of STEP delayed the onset of motor dysfunction and prevented the appearance of cognitive deficits in R6/1 mice. This phenotype was accompanied by an increase in pERK1/2 levels, a delay in the decrease of striatal DARPP-32 levels and a reduction in the size of mhtt aggregates, both in the striatum and CA1 hippocampal region. We also found that acute pharmacological inhibition of STEP with TC-2153 improved cognitive function in R6/1 mice. In conclusion, our results show that deletion of STEP has a beneficial effect on motor coordination and cognition in a mouse model of HD suggesting that STEP inhibition could be a good therapeutic strategy in HD patients.

1. Introduction

Huntington's disease (HD) is an autosomal dominant progressive neurodegenerative disorder caused by an expansion of a CAG repeat in the exon-1 of the huntingtin (htt) gene (HDCR, 1993). Htt protein has a ubiquitous expression all over the organism, and in the brain it is mostly expressed in neurons (Landwehrmeyer et al., 1995). When the mutation in the htt gene exceeds 36 CAG repeats the lengthening of the polyglutamine (polyQ) chain of htt protein alters its biological functions and induces self-association (Kremer et al., 1994). Mutant htt (mhtt) aggregates localize mainly in the nucleus of striatal and cortical neurons (Difiglia et al., 1997), being a pathological hallmark of HD.

HD patients present motor disturbances, manifested as involuntary choreiform movements, and difficulty in controlling voluntary movement mostly due to the preferential loss of GABAergic projection neurons (medium-sized spiny neurons) in the caudate nucleus and putamen (Vonsattel et al., 1985). However, lately it has been proposed that the first symptoms in HD patients are cognitive deficits, such as altered acquisition of new motor skills, planning and memory, and paired attention, which become more evident as the disease progresses. Cognitive deficits are related to the dysfunction of the corticostriatal pathway and the hippocampus (Puigdellívol et al., 2016).

Even though the molecular mechanisms underlying the pathophysiology of HD have not been fully elucidated yet, it is known that the presence of mhtt induces the disruption of the tight balance between protein phosphatases and kinases (Saavedra et al., 2011a). STriatal-En- riched protein tyrosine Phosphatase (STEP) is highly expressed in the striatum and at lower levels in the cortex, hippocampus and amygdala (Boulanger et al., 1995). It is encoded by Ptpn5 gene and alternative splicing produces four isoforms (Lombroso et al., 1991). The active and most common isoforms are the cytosolic STEP46, only expressed in the striatum, and the membrane-associated STEP61 (Boulanger et al., 1995; Bult et al., 1997). STEP regulates the phosphorylation of several sub- strates, all of them implicated in synaptic plasticity, such as ERK1/2 (Lombroso et al., 2016).

STEP levels and activity are altered in several neurodegenerative and psychiatric disorders (Karasawa and Lombroso, 2014). In HD, STEP mRNA levels are decreased in the brain of patients (Hodges et al., 2006) and its activity is decreased in the striatum,

hippocampus and cortex of HD mouse models (Saavedra et al., 2011b). Furthermore, reduced STEP activity, and consequent increased pERK1/2 levels, in the striatum of R6 mouse models of HD participates in the development of the resistance to excitotoxity, indicating that the progressive reduction of STEP in HD brain could be neuroprotective (Saavedra et al., 2011b). Indeed, the excitotoxin-sensitive YAC128 HD mouse model has increased STEP activity at striatal postsynaptic densities (Gladding et al., 2012).

In the present study, we asked whether STEP inactivation could be neuroprotective in HD. To answer this question, we evaluated the motor and cognitive effect of the genetic knock out and pharmacological inhibition of STEP in R6/1 mice. Our results show that STEP inhibition improves motor coordination and cognition in R6/1 mice.

2. Methods

2.1. Animals

Wild-type (mhtt−/− STEP+/+; WT), R6/1 (mhtt+/− STEP+/+), STEP KO (mhtt−/− STEP−/−), and R6/1 STEP KO (mhtt+/− STEP−/−) male mice were maintained in a C57BL6 background and genotyped by polymerase chain reaction as described previously (Mangiarini et al., 1996; Venkitaramani et al., 2009). Since the original background of R6/1 mice was B6CBA (Jackson Laboratory, Bar Harbor, ME), we first backcrossed them for ten generations to C57BL6 background, the same as STEP KO mice, in order to avoid background interferences. To obtain R6/1 STEP KO colony we crossed R6/1 females with STEP KO males and the resultant mhtt+/− STEP+/− heterozygous mice were crossed with STEP KO mice afterwards. Thus, WT animals were mated with R6/1 mice, obtaining both genotypes, and STEP KO mice with R6/1 STEP KO mice (Fig. S1). Our R6/1 and R6/1 STEP KO colonies have around 300 CAG re- peats in the striatum and hippocampus (Supplementary Table 1). The number of CAG repeats was analyzed using the Adellgene Huntington Disease Kit (BDR, Spain) following the manufacturer's instructions. Animals were housed in cages lined with sawdust under a standard 12/12 h light/dark cycle (lights on at 08:00 am) with food and water available ad libitum. Every effort was made to minimize animal suffering and to use the minimum number of animals per group and experiment.

2.2. Behavioral assessment

2.2.1. Body weight and clasping

Body weight and clasping were measured weekly from 8 to 24 weeks of age. Clasping was measured suspending mice from their tail and ob- serving the hind limb position for 30 s. Mice were scored according to the following criteria: 0 = no clasping, 1 = clasping two paws and 2 = clasping all paws (Anglada-Huguet et al., 2014).

2.2.2. Rotarod

Motor coordination was evaluated using the rotarod apparatus (30 mm diameter). A batch of 8-week-old animals was trained at a con- stant speed (4 rpm) until the animal remained during 60 s above the ap- paratus. Next week, mice were evaluated once a week at 16 rpm un- til they were 24 week-old. Each mouse performed three separate trials at a maximum of 180 s and the latency to fall was recorded. Different batches of mice of 8, 12, 18 and 24 weeks of age performed the accel- erating version. In this task, the rotation speed gradually increases from 4 to 40 rpm over the course of 5 min. Each animal performed 12 trials during three consecutive days and the latency to fall was recorded.

2.2.3. Novel object location test (NOLT)

The object location memory task evaluates spatial memory and is based on the ability of mice to recognize when a familiar object has been relocated. Mice (12 and 18 weeks of age) were first habituated to the arena (40 × 40 × 70 cm) in the absence of objects (2 sessions of 10 min). On the third day, during the acquisition phase, mice were allowed to explore for 10 min two duplicate objects that were placed in the far cor- ners of the arena. Four different cues were placed on the top of the wall of the arena, far enough from mice to avoid physical contact. After a de- lay of 24 h, 1 object was placed in the corner diagonally opposite. Thus, both objects in this phase were equally familiar, but one was in a new location. The position of the new object was counterbalanced between mice. The location preference was measured as the time exploring each location × 100/time exploring both locations (Anglada-Huguet et al., 2014). Animals were tracked and recorded with SMART Junior software (Panlab, Spain).

2.2.4. Novel object recognition test (NORT)

This paradigm is based on the natural tendency of mice to spend more time exploring a novel object than a familiar one. Mice (12 and 18 weeks of age) were first habituated to the arena (40 × 40 × 70 cm) in the absence of objects (2 sessions of 10 min). On the third day, two similar objects were presented to each mouse during 10 min, af- ter which they were returned to their home cage. 24 h later (long-term memory), the same animals were retested for 5 min in the arena with a familiar and a new object. The object preference was measured as the time exploring each object × 100/time exploring both objects (Anglada-Huguet et al., 2014). Animals were tracked and recorded with SMART Junior software.

2.2.5. T-maze Spontaneous Alternation Task (T-SAT)

The apparatus consisted of 3 arms (45 × 8 × 20 cm), two of them situated at 180° from each other, and the third representing the stem arm of the T, situated at 90° with respect to the other two. Two identical guillotine doors were placed in the entry of each arm. Light inten sity was 5 lx throughout the maze. In the training session, one arm was closed (new arm) and 12 and 18 week-old mice were placed in the stem arm of the T and allowed to explore this arm and the other available arm (old arm) for 10 min, after which they were returned to the home cage. After 4 h (long-term memory), mice were placed in the stem arm of the T-maze and allowed to freely explore all 3 arms for 5 min. Arm preference was determined by calculating the time spent in each arm × 100/time spent in both arms (familiar and novel) (Anglada-Huguet et al., 2014). Animals were tracked and recorded with SMART Junior soft- ware.

2.2.6. Pharmacological treatment

Twelve-week-old WT and R6/1 male mice were administered i.p. with vehicle (2% DMSO in saline) or TC-2153 (10 mg/kg) 3 h prior training sessions of NOLT and NORT, as described elsewhere (Xu et al., 2014). The same mice were used in both tests with a washout period of two days between them.

2.2.7. Total protein extraction and Western blot analysis

Animals were killed by cervical dislocation and the hippocampi and striata were rapidly removed on ice. Tissue was homogenized in lysis buffer [50 mM Tris-HCl (pH 7.5), 150 mM NaCl, 10% glycerol, 1% Triton X-100, 100 mM NaF, 5 μM ZnCl2 and 10 mM EGTA] plus protease inhibitors [phenylmethylsulphonyl fluoride (2 mM), aprotinin (1 μg/ml), leupeptin (1 μg/ml) and sodium orthovanadate (1 mM)] and centrifuged at 16,100 g for

20 min. The supernatants were collected and the protein concentration was measured using the DC protein as- say kit (Bio-Rad, Hercules, CA, USA). Western blot analysis was per- formed as previously described (Saavedra et al., 2011b). The follow- ing primary antibodies were used: anti-STEP (23E5; 1:1000), pan-ERK (1:1000), anti-phospho-ERK1/2Tyr202/Tyr204 (pERK1/2; 1:1000), all from Santa Cruz Biotechnology (Santa Cruz, CA, USA), and anti-DARPP-32 (1:1000; BD Bioscience, San Jose, CA USA). All of them were incubated overnight at 4 °C. Mouse monoclonal antibody against α-tubulin (1:50,000; Sigma, St. Louis, MO, USA) was used to obtain a loading control. After incubation with primary antibodies, membranes were washed with Tris-buffered saline containing 0.1% Tween-20 (TBS-T), incubated for 1 h (15 min for loading controls) at room temperature with the corresponding horseradish peroxidase-conjugated antibody (1:2000; Promega, Madison, WI, USA) and washed again with TBS-T. Immunoreactive bands were visualized using the Western Blotting Luminol Reagent (Santa Cruz Biotechnology) and quantified by a computer-assisted densitometer (Gel-Pro Analyzer, version 4, Media Cybernetics).

2.3. Immunohistochemistry

Coronal sections (30 µm) of the whole brain were obtained. Anti-DARPP-32 (1:1000; BD Bioscience, San Jose, CA, USA) antibody was used for free-floating immunofluorescence that was performed as described elsewhere (Rué et al., 2016). After primary antibody incuba-ion, slices were washed three times and then incubated for 2 h shaking at room temperature with Cyanine-3 anti-mouse (1:300; Jackson Im- munoResearch, West Grove, PA, USA). Nuclei were stained with DAPI – Fluoromount (SouthernBiotech, Birmingham, AL, USA). DARPP-32 striatal staining was examined and photographed at 2× using an Olympus BX60 epifluorescence microscope (Olympus, Tokyo, Japan) equipped with an Orca-ER cooled CCD camera (Hamamatsu Photonics, Hama- matsu, Japan). Anti-EM48 (1:150; Millipore, Billerica, MA, USA) anti- body was used for htt aggregates detection. Sections were incubated with biotinylated secondary antibody (1:200; Thermo Fisher, Rockford, IL, USA), and developed with Diaminobenzidine (DAB), as previously described (Anglada-Huguet et al., 2014). DARPP-32 and EM48 stainings were examined in 8 slices per animal separated by 240 µm (covering the entire striatum or CA1 hippocampal regions) by using Computer-Assisted Stereology Toolbox (CAST) software (Olympus Danmark A/S). All images were analyzed using CellProfiler Analyst software (Jones et al., 2008).

2.4. Statistical analysis

All data are expressed as mean ± SEM. Different statistical analyses were performed with Prism 5.0 (GraphPad Software, La Jolla, CA, USA) using the Student's t-test or the one- or two-way ANOVA, followed by Bonferroni's post hoc test as appropriate and indicated in the figure leg- ends. Any value lower or higher than two times standard deviation away from the mean was considered an outlier and was excluded from the study. Values of $p < .05$ were considered statistically significant (95% confidence).

3. Results

3.1. Lack of STEP delays motor coordination dysfunction and DARPP-32 levels reduction in R6/1 mice

It has been widely reported that HD mice present motor coordination impairment in the rotarod test (Puigdellívol et al., 2016). Therefore, we analyzed motor coordination from 8 to 24 weeks of age in all the genotypes. Our data confirmed that R6/1 mice presented a progressive motor dysfunction with an onset at 15 weeks of age (Fig. 1A). Interestingly, R6/1 STEP KO mice did not show significant motor coordination impairment until 19 weeks of age (Fig. 1A). We also analyzed motor learning at 8, 12, 18 and 24 weeks of age by using the accelerating rotarod test. Our results showed that all genotypes performed similarly this task at 8 and 12 weeks of age (Fig. S2A). However, R6/1, but not R6/1 STEP KO mice, presented a severe motor dysfunction at 18 weeks of age when compared with WT and STEP KO mice (Fig. 1B). At 24 weeks of age, both R6/1 and R6/1 STEP KO mice presented statistically significant worse performance compared with WT and STEP KO mice (Fig. 1B). Al- though STEP is a striatal-enriched protein, we did not find alterations in the fixed or accelerating rotarod in STEP KO mice at any age tested (Fig. 1A, B) in line with previous studies (Venkitaramani et al., 2011). In parallel, we measured body weight and clasping neurological reflex. Our data showed that R6/1 and R6/1 STEP KO mice presented a significant reduction of their body weight during the studied period compared with WT and STEP KO mice (Fig. S2B). However, R6/1 mice started presenting this phenotype at week 12th, one week earlier than R6/1 STEP KO mice. In the same way, both R6/1 groups presented clasping neuro- logical reflex, an indicative of neurological

dysfunction, but R6/1 STEP KO mice developed this phenotype later than R6/1 mice (Fig. S2C).

Next, we analyzed the molecular consequences of the lack of STEP activity in the striatum. First, we confirmed the absence of STEP46 and STEP61 in the striatum of STEP KO and R6/1 STEP KO mice, and we detected the decrease of both isoforms levels in the striatum of R6/1 mice at 12, 18 and 24 weeks of age (Fig. S3) as previously described (Saavedra et al., 2011b). As a readout of the lack of STEP activity, we analyzed the levels of pERK1/2, one of the substrates of STEP. We observed increased pERK1/2 levels in the striatum of STEP KO and R6/1 STEP KO mice from 12 to 24 weeks of age (Fig. 1C).

We also analyzed DARPP-32, a striatal medium-sized spiny neurons marker, whose levels are reduced in HD mice from early stages of the disease (Bibb et al., 2000). Western blot results showed that R6/1 mice presented a significant decrease in DARPP-32 levels in all the ages an- alyzed when compared with WT and STEP KO mice (Fig. 1D). Inter- estingly, in R6/1 STEP KO mice the decrease in DARPP-32 levels was delayed since it was detected from 18 weeks of age onwards (Fig. 1D). In addition, 18 week-old double mutant animals showed significantly higher DARPP-32 levels compared to R6/1 mice (Fig. 1D). Addition- ally, we analyzed striatal DARPP-32 mean intensity and striatal volume by immunohistochemistry. As observed by Western blot, R6/1 mice dis- played a significant reduction of DARPP-32 mean intensity in all the ages analyzed in comparison to WT and STEP KO mice (Fig. 1E). In contrast, DARPP-32 mean intensity in double mutant mice was only significantly reduced at 24 weeks of age compared with WT and STEP KO mice (Fig. 1E). Striatal volume was similar in all the genotypes and ages analyzed (Fig. S4).

3.2. Lack of STEP improves hippocampal-dependent cognitive function and increases hippocampal pERK1/2 levels in R6/1 mice

As previously described by our group, R6/1 mice show long-term memory (LTM) deficits in recognition and spatial memory from 12 weeks of age (Giralt et al., 2011). In order to determine the effect of constitutive STEP genetic deletion on the cognitive ability of R6/1 mice, we performed the NOLT, NORT and T-SAT. We started evaluating cognition at 12 weeks of age. In the NOLT and NORT, during the training session all mice explored equally the two identical objects (A and A'), indicating no object preference (Fig. S5). During the test session in the NOLT and NORT, WT, STEP KO and R6/1 STEP KO mice explored

significantly more time the object that was re-located or changed, while R6/1 mice did not show significant preference for the new object/lo- cation (Fig. 2A). Similarly, in the T-SAT, the analysis of the time spent exploring the familiar and the novel arm showed that WT, STEP KO and R6/1 STEP KO mice spent significantly more time in the novel arm than in the familiar one, whereas R6/1 mice explored both equally (Fig. 2A). To analyze whether the cognitive improvement observed in 12 week-old R6/1 STEP KO mice was maintained or lost at later stages, we tested cognition at 18 weeks of age. Since our previous results al- ready showed hippocampal-dependent memory deficits in R6/1 mice at 12 weeks of age, we only tested cognition at 18 weeks of age in double mutant mice, and compared them to STEP KO mice as controls. As previously described (Venkitaramani et al., 2011), we observed that STEP KO mice had preserved memory since they explored significantly more time the re-located object in the NOLT, the novel one in the NORT and the new arm in the T-SAT (Fig. 2B). Interestingly, R6/1 STEP KO mice
also presented conserved memory in these three tests (Fig. 2B).

After confirming the absence of STEP61 in the hippocampus of STEP KO and R6/1 STEP KO mice (Fig. S6A), we next analyzed pERK1/2, a key STEP substrate in LTM formation (Adams and Sweatt, 2002). No significant differences in basal pERK1/2 levels were detected between genotypes at 12 and 18 weeks of age (Fig. S6B). However, when analyzing the levels in those animals subjected to cognitive tests at 12 weeks, sacrificed 1 h after the T-SAT, we found an increase of 38.91 ± 12.24% in pERK1/2 levels in R6/1 STEP KO mice compared with R6/1 mice (Fig. 2A). Regarding those animals subjected to cognitive tests at 18 weeks of age, we observed similar pERK1/2 levels in STEP KO and R6/1 STEP KO mice (Fig. 2B).

3.3. Lack of STEP reduces mhtt aggregate size in R6/1 mice

Since the presence of mhtt aggregates is the principal hallmark of HD (Difiglia et al., 1997), we analyzed whether the lack of STEP could affect their presence in the striatum and hippocampus of R6/1 mice. We found that R6/1 STEP KO mice, in comparison to R6/1 mice, presented a reduction in the mean area (Fig. 3A), but not in the density (Fig. 3C), of striatal mhtt aggregates at all the ages analyzed. Similarly, in CA1 hippocampal region mhtt aggregates were smaller in R6/1 STEP KO in comparison to R6/1 mice at 12

and 18 weeks of age (Fig. 3B). Regarding mhtt aggregates density in this region, there was a significant decrease at 12 weeks of age in double mutant mice compared to R6/1. Neverthe- less, this difference was lost at 18 weeks of age (Fig. 3D).

3.4. Acute STEP inhibition improves hippocampal-dependent memory in R6/1 mice

To investigate whether an acute inhibition of STEP could repro- duce the cognitive improvements found when STEP was genetically removed, we used TC-2153, a highly specific STEP inhibitor (Xu et al., 2014). We treated 12 week-old WT and R6/1 mice with 10 mg/kg TC-2153 i.p. 3 h prior the training sessions of NOLT and NORT. No object preference was observed in the training session of both NOLT and NORT (Fig. S7). In the testing sessions, we found that WT mice, independently of the treatment received, explored significantly more time the new location/object in the NOLT and NORT. On the other hand, and as expected, vehicle-treated R6/1 mice were not able to discern between the old and the new object/location and explored equally both objects in the two tests. Interestingly, R6/1 mice treated with TC-2153 showed preserved memory and explored significantly more time the new location and object in the NOLT and NORT, respectively (Fig. 4).

4. Discussion

In the present study, we show that the genetic lack of STEP delays motor coordination and learning impairment and prevents hippocampal-dependent cognitive deficits in the R6/1 mouse model of HD. In addition, the acute pharmacological inhibition of STEP also improves cognitive ability in R6/1 mice.

Here we found that genetic deletion of STEP in the R6/1 mouse model had a slightly beneficial effect on body weight and clasping re- flex, since R6/1 STEP KO mice presented alterations one week later than R6/1 mice. This time course of body weight loss was similar to that previously described in transgenic R6/1 mice in hybrid (CBA x C57BL6) (Clifford et al., 2002; Dowie et al., 2010) and inbred (C57BL6) (Brooks et al., 2012) background. Since STEP is a neural protein, it is not surprising to find only a little effect on body weight in those animals lacking this protein. Regarding clasping reflex, our C57BL6 R6/1 mice started presenting this alteration at 12 weeks of age, slightly before

than previously reported for R6/1 hybrid mice (Anglada-Huguet et al., 2014; Mangiarini et al., 1996).

Remarkably, we found that lack of STEP notably delayed the on-set of motor dysfunction in HD mice as shown by the performance of R6/1 STEP KO mice in the rotarod. While R6/1 mice started to present deficits in motor coordination at 12–13 weeks of age in the fixed rotatod, earlier than previously described for R6/1 hybrid mice (Anglada-Huguet et al., 2014), it was not until 19 weeks of age when the double mutant mice started performing worse. Similarly, at the accelerating rotarod, R6/1 presented deficits in motor learning at 18 weeks of age, but it was not until 24 weeks of age when R6/1 STEP KO mice showed alterations in this task. As previously reported (Venkitaramani et al., 2011), STEP KO mice did not present alterations in motor tasks, since their performance in fixed and accelerating rotarod was comparable to those of WT. Altogether, these results suggest that the lack of STEP delays the onset of alterations in motor coordination and motor learning in R6/1 mice.

In addition to this phenotype, we observed a constitutive increase of pERK1/2 levels in the striatum of R6/1 STEP KO mice. Accordingly, a recent work supports that the inhibition of STEP, and the consequent increase in the phosphorylation of its substrates, including pERK1/2, is beneficial for motor learning (Chagniel et al., 2014). On the other hand, we found a decrease of DARPP-32 levels in R6/1 mice at all the ages analyzed, consistent with previous studies showing decreased DARPP-32 levels as a hallmark of striatal degeneration in HD (Bibb et al., 2000; Rué et al., 2016; Vonsattel et al., 1985). In contrast, the levels of striatal DARPP-32 in double mutant mice were maintained until 18 weeks of age, a week before the onset of motor deficits in the rotarod. Interestingly, we observed a reduction in the size of mhtt aggregates in the striatum of double mutant mice. Previous studies have described a correlation between the reduction in the size of mhtt aggregates and motor improvement in pharmacologically treated (Anglada-Huguet et al., 2014; Chen et al., 2011) and genetically manipulated (Yang et al., 2017) HD mouse models. Altogether, our results suggest that lack of STEP induces a general improvement in striatal neuronal function through the decrease in the size of mhtt aggregates, increased pERK1/2 levels and the maintenance of DARPP-32 protein levels. How- ever, it is not enough to counteract the accumulative toxic effects of mhtt and striatal medium-

sized spiny neurons finally become dysfunctional, as indicated by decreased DARPP-32 levels at 18 weeks of age and the appearance of motor symptoms.

Regarding hippocampal-dependent memory, we found that STEP KO mice performed similar to WT mice in NOLT, NORT and T-SAT, as previously described (Zhang et al., 2010). Interestingly, STEP deletion prevented LTM deficits in R6/1 mice at 12 weeks of age, when this mouse model already presents cognitive dysfunction. In order to elucidate whether this was a permanent improvement or a delay in the on- set of the deficits, we tested cognition at 18 weeks of age. The present results and data in the literature have already shown that R6/1 mice present hippocampal-dependent cognitive dysfunction from 12 weeks of age (Anglada-Huguet et al., 2014; Giralt et al., 2011; Saavedra et al., 2013). Thus, we only tested cognition in R6/1 STEP KO mice and com- pared them to STEP KO mice as controls. Interestingly, we also found an intact cognitive ability in the double mutant mice, suggesting that lack of STEP prevents the appearance of cognitive symptoms at least until 18 weeks of age in R6/1 mice. Our results are in accordance with previous studies showing an important role of STEP in learning and memory function (Fitzpatrick and Lombroso, 2011; Venkitaramani et al., 2009, 2011). In addition, the genetic reduction of STEP has been proved to prevent cognitive deficits in a mouse model of Alzheimer's disease (AD) (Zhang et al., 2010). Thus, low levels of STEP appear to be beneficial in HD more than participating in the pathophysiology.

In correlation with cognitive improvement in hippocampal-dependent tasks, we observed increased hippocampal pERK1/2 levels in double mutant mice after cognitive tests. In line with our results, a previous study (Venkitaramani et al., 2011) showed a correlation between increased hippocampal pERK1/2 levels and enhanced performance of STEP KO mice in hippocampal-dependent learning and memory tasks (Morris and radial-arm water mazes), reinforcing the importance of ERK1/2 phosphorylation in memory formation. In fact, decreased levels of hippocampal pERK1/2 have been related to impaired memory in a mouse model of chronic stress and in a rat model of focal cerebral ischemia (Li et al., 2016, 2017). Those deficits could be rescued by in- creasing phosphorylation of ERK1/2 with different pharmacological approaches (Li et al., 2016; Yabuki et al., 2015). Moreover, phosphorylation levels of ERK1/2 have been also associated to age-related cognitive decline (Hu et al., 2015).

In addition to increased pERK1/2 levels, we also found a reduction in the size of mhtt aggregates in the CA1 hippocampal region. Importantly, this region is critical for new memory formation (Remondes and Schuman, 2004; Tsien et al., 1996). In this line, it has been shown that post-hypoxic damage in CA1 results in memory impairments (Li et al., 2016), whereas alterations in cognitive function in AD and HD have been related to CA1 atrophy and synaptic alterations, respectively (Bulley et al., 2012; Kerchner et al., 2012; Murphy et al., 2000). In fact, pharmacological treatment with a prostaglandin E2 EP1 receptor antagonist reduced the number of mhtt aggregates in the CA1 hippocampal region and improved memory alterations in R6/1 mice (Anglada-Huguet et al., 2014). This suggests that the smaller size of mhtt aggregates may improve synaptic function in the CA1 region, playing a role, together with the increase in pERK1/2 levels, in the preservation of memory in double mutant mice.

How STEP deletion results in a reduction in the size of mhtt aggregates is not clear, but it seems to be an indirect effect. Indeed, we observed that the size of mhtt aggregates in striatum, a STEP-enriched region, and in CA1 hippocampal region, where STEP expression is not particularly enriched (Kohara et al., 2014; Shinohara et al., 2012), is equally modulated by the deletion of STEP. This suggests that the bio- chemical changes observed in both regions result in an overall wellbeing of the cells that allows them to better process the mhtt aggregates. In this line, the improvement in biochemical parameters and cognitive function in a mouse model of AD with genetic deletion of STEP was not associated with an increased clearance of amyloid plaques (Zhang et al., 2010). Interestingly, we show that not only genetic knock out of STEP, but also pharmacological inhibition of its activity, improved LTM performance in 12 week-old R6/1 mice. These results are in accordance with previous studies describing a beneficial role of TC-2153 on memory in mouse models of AD and schizophrenia (Xu et al., 2015, 2014). Thus, taken together, our results suggest that STEP inhibition produces a mnemonic effect in R6/1 mice.

5. Conclusion

Here, we show that deletion of STEP has a beneficial role on motor alterations and cognitive deficits in HD, suggesting that the decreased levels and/or activity previously

found in the brain of HD mouse models do not take part in the pathophysiology, but are beneficial instead. In addition, our results showing that acute inhibition of STEP activity im- proves cognitive function suggest that lowering of STEP activity could be a therapeutic intervention for HD patients.

Acknowledgements

This work was supported by the project PI13/01250 integrado en el Plan Nacional de I+D+I y cofinanciado por el ISCIII-Subdirección Gen- eral de Evaluación y el Fondo Europeo de Desarrollo Regional (FEDER), and grants SAF2016-08573-R (to E.P.-N.) and SAF2017-88076-R (to J.A,) from Ministerio de Economia y Competitividad, Spain. We are very grateful to Dr. Paul J. Lombroso (Yale University School of Medicine, New Haven, Connecticut, USA) for the generous gift of STEP knock out mice and STEP inhibitor TC-2153 and Dr. Ana Saavedra (University of Barcelona) for critical reading of the manuscript. We also thank Ana López, M. Teresa Muñoz, Dr. Teresa Rodrigo, Dr. Lara Sedó and the staff of the animal facility from the Faculty of Psychology and Medicine (University of Barcelona, Barcelona) for their technical support.

References

Adams, J.P., Sweatt, J.D., 2002. Roles for the ERK MAP kinase cascade in memory. Annu. Rev. Pharmacol. Toxicol. 42, 135–163.

Anglada-Huguet, M., Xifró, X., Giralt, A., Zamora-Moratalla, A., Martín, E.D., Alberch, J., 2014. Prostaglandin E2 EP1 receptor antagonist improves motor deficits and rescues memory decline in R6/1 mouse model of Huntington's disease. Mol. Neurobiol. 49, 784–795.

Bibb, J.A., Yan, Z., Svenningsson, P., Snyder, G.L., Pieribone, V.A., Horiuchi, A., Nairn, A.C., Messer, A., Greengard, P., 2000. Severe deficiencies in dopamine signaling in presymptomatic Huntington's disease mice. Proc. Natl. Acad. Sci. 97, 6809–6814.

Boulanger, L.M., Lombroso, P.J., Raghunathan, a, During, M.J., Wahle, P., Naegele, J.R., 1995. Cellular and molecular characterization of a brain-enriched protein tyrosine phosphatase. J. Neurosci. 15, 1532–1544.

Brooks, S.P., Janghra, N., Workman, V.L., Bayram-Weston, Z., Jones, L., Dunnett, S.B., 2012. Longitudinal analysis of the behavioural phenotype in R6/1 (C57BL/6J) Huntington's disease transgenic mice. Brain Res. Bull. 88, 94–103.

Bulley, S.J., Drew, C.J.G., Morton, A.J., 2012. Direct visualisation of abnormal dendritic spine morphology in the hippocampus of the R6/2 transgenic mouse model of Huntington's disease. J. Huntingtons. Dis. 1, 267–273.

Bult, A., Zhao, F., Dirkx, R.J., Raghunathan, A., Solimena, M., Lombroso, P.J., 1997. STEP: a family of brain-enriched PTPs. Alternative splicing produces transmembrane, cytosolic and truncated isoforms. Eur. J. Cell Biol. 72, 337–344.

Chagniel, L., Bergeron, Y., Bureau, G., Massicotte, G., Cyr, M., 2014. Regulation of tyrosine phosphatase STEP61 by protein kinase a during motor skill learning in mice. PLoS One 9, 1–8.

Chen, X., Wu, J., Lvovskaya, S., Herndon, E., Supnet, C., Bezprozvanny, I., 2011. Dantrolene is neuroprotective in Huntington's disease transgenic mouse model. Mol. Neurodegener. 6, 81.

Clifford, J.J., Drago, J., Natoli, A.L., Wong, J.Y.F., Kinsella, A., Waddington, J.L., Vaddadi, K.S., 2002. Essential fatty acids given from conception prevent topographies of motor deficit in a transgenic model of Huntington's disease. Neuroscience 109, 81–88.

Difiglia, M., Sapp, E., Chase, K.O., Davies, S.W., Bates, G.P., Vonsattel, J.P., Aronin, N., 1997. Aggregation of huntingtin in neuronal intranuclear inclusions and dystrophic neurites in brain. Science (80-) 277, 1990–1993.

Dowie, M.J., Howard, M.L., Nicholson, L.F.B., Faull, R.L.M., Hannan, A.J., Glass, M., 2010. Behavioural and molecular consequences of chronic cannabinoid treatment in Huntington's disease transgenic mice. Neuroscience 170, 324–336.

Fitzpatrick, C.J., Lombroso, P.J., 2011. The role of striatal-enriched protein tyrosine phosphatase (STEP) in cognition. Front. Neuroanat. 5, 1–11.

Giralt, A., Saavedra, A., Carretón, O., Xifró, X., Alberch, J., Pérez-Navarro, E., 2011. Increased PKA signaling disrupts recognition memory and spatial memory: Role in Huntington's disease. Hum. Mol. Genet. 20, 4232–4247.

Gladding, C.M., Sepers, M.D., Xu, J., Zhang, L.Y.J., Milnerwood, A.J., Lombroso, P.J., Raymond, L.A., 2012. Calpain and STriatal-Enriched protein tyrosine Phosphatase (STEP) activation contribute to extrasynaptic NMDA receptor localization in a huntington's disease mouse model. Hum. Mol. Genet. 21, 3739–3752.

HDCR, 1993. A novel gene containing a trinucleotide repeat that is expanded and unstable on Huntington's disease chromosomes. The Huntington's Disease Collaborative Research Group. Cell 72, 971–983.

Hodges, A., Strand, A.D., Aragaki, A.K., Kuhn, A., Sengstag, T., Hughes, G., Elliston, L.A., Hartog, C., Goldstein, D.R., Thu, D., Hollingsworth, Z.R., Collin, F., Synek, B., Hol- mans, P.A., Young, A.B., Wexler, N.S., Delorenzi, M., Kooperberg, C., Augood, S.J., Faull, R.L.M., Olson, J.M., Jones, L., Luthi-Carter, R., 2006. Regional and cellular gene expression changes in human Huntington's disease brain. Hum. Mol. Genet. 15, 965–977.

Hu, A., Yuan, H., Wu, L., Chen, R., Chen, Q., Zhang, T., Wang, Z., Liu, P., Zhu, X., 2015. The effect of constitutive over-expression of insulin-like growth factor 1 on the cogni- tive function in aged mice. Brain Res. 1631, 1–10.

Jones, T.R., Kang, I.H., Wheeler, D.B., Lindquist, R.A., Papallo, A., Sabatini, D.M., Golland, P., Carpenter, A.E., 2008. CellProfiler Analyst: Data exploration and analysis software for complex image-based screens. BMC Bioinformatics 9, 1–16.

Karasawa, T., Lombroso, P.J., 2014. Disruption of striatal-enriched protein tyrosine phosphatase (STEP) function in neuropsychiatric disorders. Neurosci. Res. 89, 1–9.

Kerchner, G.A., Deutsch, G.K., Zeineh, M., Dougherty, R.F., Saranathan, M., Rutt, B.K., 2012. Hippocampal CA1 apical neuropil atrophy and memory performance in Alzheimer's disease. NeuroImage 63, 194–202.

Kohara, K., Pignatelli, M., Rivest, A.J., Jung, H.Y., Kitamura, T., Suh, J., Frank, D., Ka- jikawa, K., Mise, N., Obata, Y., Wickersham, I.R., Tonegawa, S., 2014. Cell type-spe- cific genetic and optogenetic tools reveal hippocampal CA2 circuits. Nat. Neurosci. 17, 269–279.

Kremer, B., Goldberg, P., Andrew, S.E., Theilmann, J., Telenius, H., Zeisler, J., Squitieri, F., Lin, B., Bassett, A., Almqvist, E., 1994. A worldwide study of the Huntington's dis- ease mutation. The sensitivity and specificity of measuring CAG repeats. N. Engl. J. Med. 330, 1401–1406.

Landwehrmeyer, G.B., McNeil, S.M., Dure, L.S., Ge, P., Aizawa, H., Huang, Q., Ambrose, C.M., Duyao, M.P., Bird, E.D., Bonilla, E., de Young, M., Avila-Gonzales, A.J., Wexler,

N.S., Difiglia, M., Gusella, J.F., MacDonald, M.E., Penney, J.B., Young, A.B., Vonsat- tel, J.-P., 1995. Huntington's disease gene: regional and cellular expression in brain of normal and affected individuals. Ann. Neurol. 37, 218–230.

Li, Z., Fang, F., Wang, Y., Wang, L., 2016. Resveratrol protects CA1 neurons against focal cerebral ischemic reperfusion-induced damage via the ERK-CREB signaling pathway in rats. Pharmacol. Biochem. Behav. 146–147, 21–27.

Li, Y., Chen, Y., Gao, X., Zhang, Z., 2017. The behavioral deficits and cognitive impairment are correlated with decreased IGF-II and ERK in depressed mice induced by chronic unpredictable stress. Int. J. Neurosci. 127, 1096–1103.

Lombroso, P.J., Murdoch, G., Lerner, M., 1991. Molecular characterization of a protein- ty- rosine-phosphatase enriched in striatum. Proc. Natl. Acad. Sci. U. S. A. 88, 7242–7246.

Lombroso, P.J., Ogren, M., Kurup, P., Nairn, A.C., 2016. Molecular underpinnings of neu- rodegenerative disorders: striatal-enriched protein tyrosine phosphatase signaling and synaptic plasticity. F1000Research 5, 2932.

Mangiarini, L., Sathasivam, K., Seller, M., Cozens, B., Harper, A., Hetherington, C., Law- ton, M., Trottier, Y., Lehrach, H., Davies, S.W., Bates, G.P., 1996. Exon 1 of the HD gene with an expanded 87, 493–506.

Murphy, K.P., Carter, R.J., Lione, L.A., Mangiarini, L., Mahal, A., Bates, G.P., Dunnett, S.B., Morton, A.J., 2000. Abnormal synaptic plasticity and impaired spatial cognition in mice

transgenic for exon 1 of the human Huntington's disease mutation. J. Neurosci. 20, 5115–5123.

Puigdellívol, M., Saavedra, A., Pérez-Navarro, E., 2016. Cognitive dysfunction in Huntington's disease: mechanisms and therapeutic strategies beyond BDNF. Brain Pathol. 26, 752–771.

Remondes, M., Schuman, E.M., 2004. Role for a cortical input to hippocampal area CA1 in the consolidation of a long-term memory. Nature 431, 699–703.

Rué, L., Bañez-Corone, M., Creus-Muncunill, J., Giralt, A., Alcalá-Vida, R., Mentxaka, G., Kagerbauer, B., Zomeño-Abellán, M.T., Aranda, Z., Venturi, V., Pérez-Navarro, E., Es- tivill, X., Martí, E., 2016. Targeting CAG repeat RNAs reduces Huntington's disease phenotype independently of Huntingtin levels. J. Clin. Invest. 126, 4319–4330.

Saavedra, Alberch, J., Pérez-navarro, E., 2011. Don't take away my p : phosphatases as therapeutic targets in Huntington's disease. Huntington's dis. - core concepts. Curr. Adv.

Saavedra, A., Giralt, A., Rue, L., Xifro, X., Xu, J., Ortega, Z., et al., 2011. Striatal-enriched protein tyrosine phosphatase expression and activity in Huntington's disease: a STEP in the resistance to excitotoxicity. J. Neurosci. 31, 8150–8162.

Saavedra, A., Giralt, A., Arumí, H., Alberch, J., Pérez-Navarro, E., 2013. Regulation of Hippocampal cGMP Levels as a Candidate to Treat Cognitive Deficits in Huntington's Disease. PLoS One 8, 1–10.

Shinohara, Y., Hosoya, A., Yahagi, K., Ferecskó, A.S., Yaguchi, K., Sík, A., Itakura, M., Takahashi, M., Hirase, H., 2012. Hippocampal CA3 and CA2 have distinct bilateral innervation patterns to CA1 in rodents. Eur. J. Neurosci. 35, 702–710.

Tsien, J.Z., Huerta, P.T., Tonegawa, S., 1996. The essential role of hippocampal CA1 NMDA receptor-dependent synaptic plasticity in spatial memory. Cell 87, 1327–1338.

Venkitaramani, D.V., Paul, S., Zhang, Y., Kurup, P., Ding, L.I., Tressler, L., Allen, M., Sacca, R., Picciotto, M.R., Lombroso, P.J., 2009. Knockout of STriatal enriched protein tyro- sine phosphatase in mice results in increased ERK1/2 phosphorylation. Synapse 63, 69–81.

Venkitaramani, D.V., Moura, P.J., Picciotto, M.R., Lombroso, P.J., 2011. Striatal-enriched protein tyrosine phosphatase (STEP) knockout mice have enhanced hippocampal memory. Eur. J. Neurosci. 33, 2288–2298.

Vonsattel, J.-P., Myers, R.H., Stevens, T.J., Ferrante, R.J., Bird, E.D., Richardson, E.P., 1985. Neuropathological classification of Huntinqton's disease. J. Neuropathol. Exp. Neurol. 44, 559–577.

Xu, J., Chatterjee, M., Baguley, T.D., Brouillette, J., Kurup, P., Ghosh, D., Kanyo, J., Zhang, Y., Seyb, K., Ononenyi, C., Foscue, E., Anderson, G.M., Gresack, J., Cuny,

G.D., Glicksman, M.A., Greengard, P., Lam, T.K.T., Tautz, L., Nairn, A.C., Ellman, J.A., Lombroso, P.J., 2014. Inhibitor of the tyrosine phosphatase STEP reverses cognitive deficits in a mouse model of Alzheimer's disease. PLoS Biol. 12, e1001923.

Xu, J., Kurup, P., Baguley, T.D., Foscue, E., Ellman, J.A., Nairn, A.C., Lombroso, P.J., 2015. Inhibition of the tyrosine phosphatase STEP61 restores BDNF expression and reverses motor and cognitive deficits in phencyclidine-treated mice. Cell. Mol. Life Sci. 73, 1503–1514.

Yabuki, Y., Shinoda, Y., Izumi, H., Ikuno, T., Shioda, N., Fukunaga, K., 2015. Dehydroepiandrosterone administration improves memory deficits following transient brain ischemia through sigma-1 receptor stimulation. Brain Res. 1622, 102–113.

Yang, S., Chang, R., Yang, H., Zhao, T., Hong, Y., Kong, H.E., Sun, X., Qin, Z., Jin, P., Li, S., Li, X., 2017. CRISPR / Cas9-mediated gene editing ameliorates neurotoxicity in mouse model of Huntington ’ s disease. J. Clin. Invest. 127, 1–6.

Zhang, Y., Kurup, P., Xu, J., Carty, N., Fernandez, S.M., Nygaard, H.B., Pittenger, C., Greengard, P., Strittmatter, S.M., Nairn, A.C., Lombroso, P.J., 2010. Genetic re- duction of striatal-enriched tyrosine phosphatase (STEP) reverses cognitive and cel- lular deficits in an Alzheimer's disease mouse model. Proc. Natl. Acad. Sci. 107, 19014–19019.

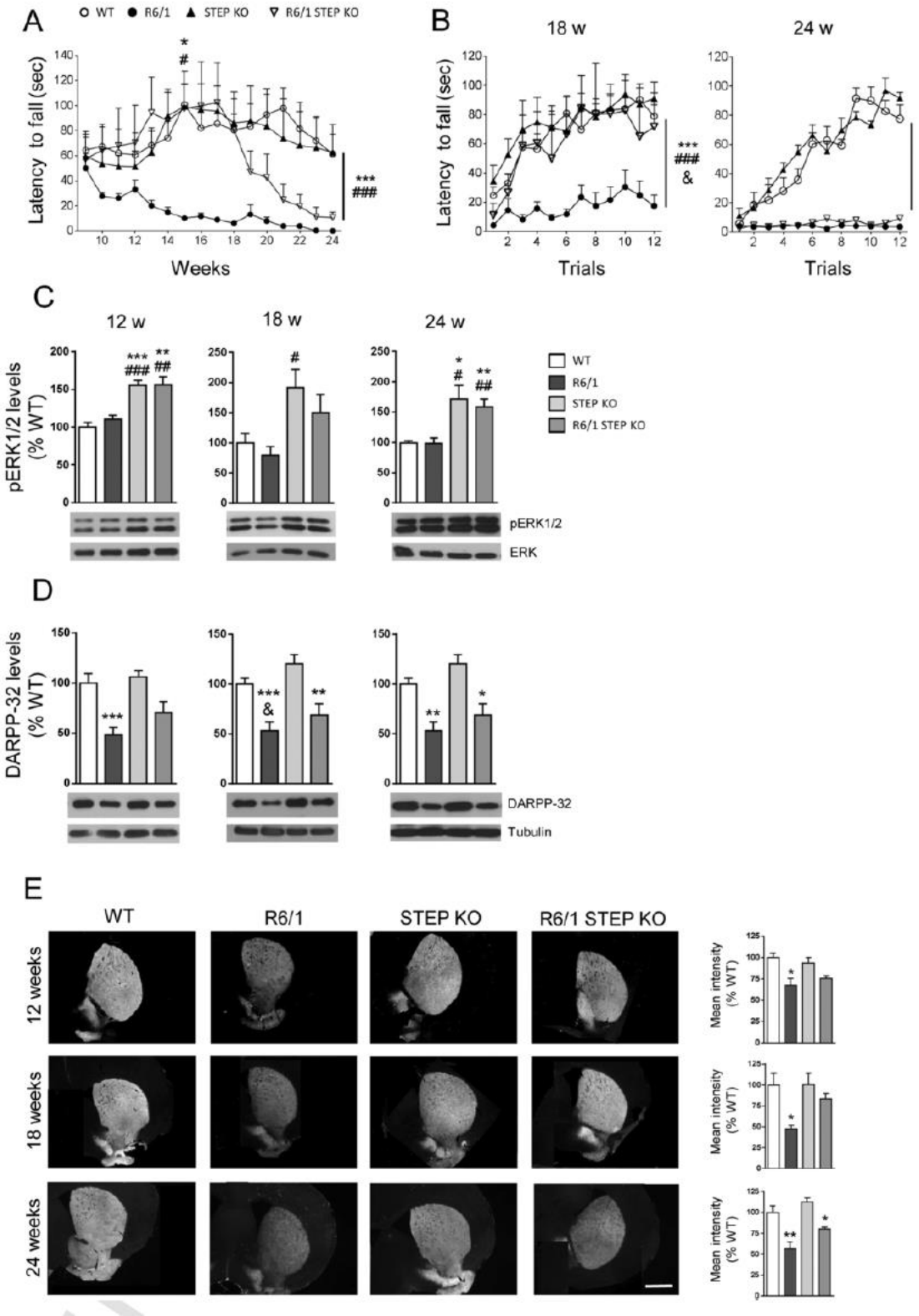

Fig. 1. Motor dysfunction and striatal DARPP-32 reduction are delayed in R6/1 STEP KO mice. The rotarod task (A) was performed weekly, at 16 rpm, in all groups from 9 to 24 weeks of age (WT n = 11; R6/1 n = 9; STEP KO n = 9 and R6/1 STEP KO n = 8). The accelerating rotarod task (B) was performed at 18 (WT n = 14; R6/1 n = 10; STEP KO n =

9 and R6/1 STEP KO n = 8) and 24 (all genotypes n = 8) weeks of age. The latency to fall is expressed as mean ± SEM. pERK1/2Tyr202/Tyr204 (C) and DARPP-32 (D) protein levels were analyzed in the striatum of mice at 12 (n = 11 per genotype), 18 (n = 9 per genotype) and 24 (n = 6 per genotype) weeks of age. Values obtained by densitometric analysis are expressed as percentage of WT mice and are shown as mean ± SEM. Representative immunoblots are shown. (E) Representative images showing DARPP-32 immunoreactivity in the striatum of all genotypes at different ages. Scale bar 1000 µm. Graphs show the mean fluorescence intensity of DARPP-32 in all genotypes at 12, 18 and 24 weeks of age. Results are expressed as a percentage of WT and are shown as mean ± SEM (n = 3–4 for each genotype and age). Data were analyzed by two-way ANOVA with Bonferroni's as a post hoc. *p < .05 and ***p < .001 versus WT and STEP KO mice (A, B, C and D); #p < .05 and ###p < .001 versus R6/1 mice (A, B and C); &p < .05 versus R6/1 STEP KO mice (b and d). *p < .05, **p < .01 and *** p < .001 versus WT mice (C).

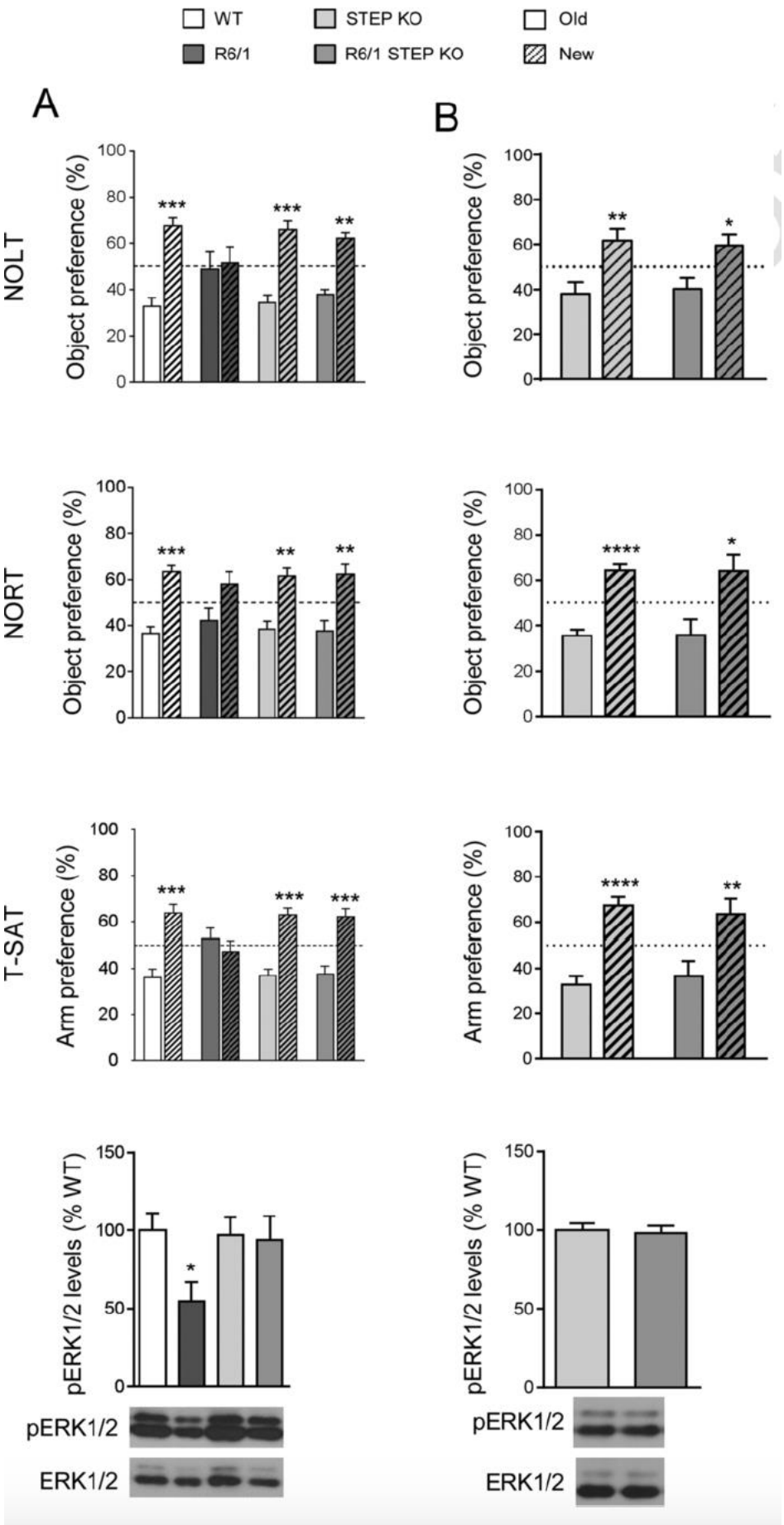
WT
R6/1
STEP KO
R6/1 STEP KO
Old
New
A
B
NOLT
NORT
T-SAT
Object preference (%)
Arm preference (%)
pERK1/2 levels (% WT)
pERK1/2
ERK1/2

Fig. 2. R6/1 STEP KO mice show improved hippocampal-dependent cognitive function. NOLT, NORT and T-SAT were used to analyze cognitive function in 12 week-old (A) WT, R6/1, STEP and R6/1 STEP KO mice and in 18 week-old (B) STEP KO and R6/1 STEP KO mice. Graphs show the percentage of preference for the object (NOLT and NORT) and the arm (T-SAT). Bars represent mean ± SEM (n = 11 for WT; n = 9 for R6/1; n = 7 for STEP KO; n = 5 for R6/1 STEP KO). pERK1/2Tyr202/Tyr204 levels were analyzed by Western blot of protein extracts obtained from the hippocampus of all genotypes subjected to cognitive tests at 12 (A) and 18 (B) weeks of age. Representative immunoblots are shown. Data were analyzed by two-way ANOVA with Bonferroni's as a post hoc (A) and Student's t-test (B). *p < .05; **p < .01; ***p < .001; ****p < .0001 compared to old object/location (in NOLT and NORT), to old arm (T-SAT) or to WT, STEP KO and R6/1 STEP KO mice (pERK1/2 levels).

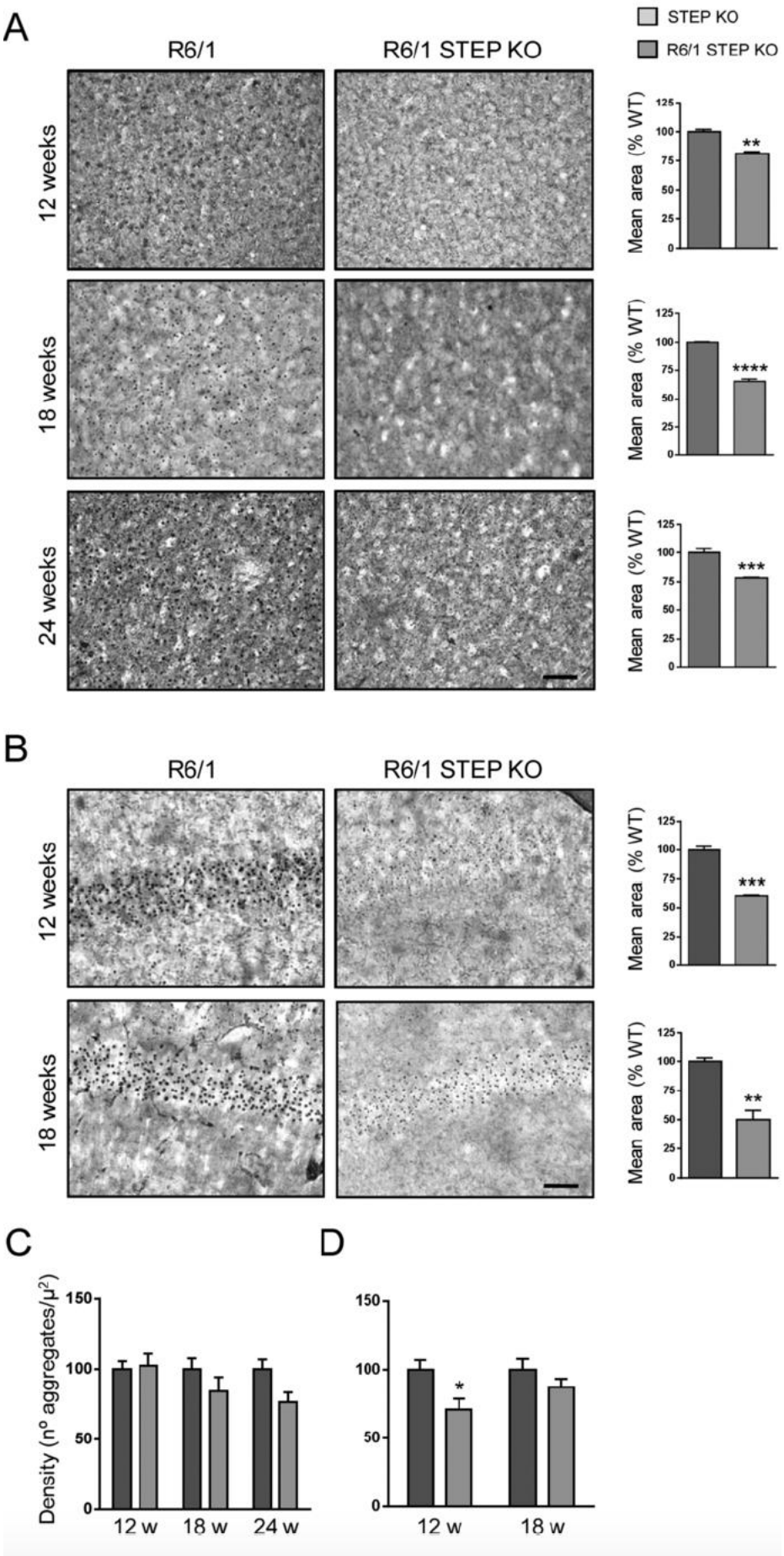
A
R6/1
R6/1 STEP KO
STEP KO
R6/1 STEP KO
12 weeks
18 weeks
24 weeks
Mean area (% WT)
125
100
75
50
25
0
**
****
***
B
R6/1
R6/1 STEP KO
12 weeks
18 weeks
Mean area (% WT)
***
**
C
Density (n° aggregates/μ²)
150
100
50
0
12 w
18 w
24 w
D
150
100
50
0
*
12 w
18 w

Fig. 3. The size of striatal and hippocampal mhtt aggregates is reduced in R6/1 STEP KO mice. Mhtt aggregates were analyzed by immunohistochemistry in 12, 18, and 24 week-old R6/1 and R6/1 STEP KO mice striatum (A, C) and hippocampus (B, D). Representative images are shown. Scale bar 50 µm. (A, B) Graphs show the mean area and (C, D) the density of mhtt aggregates expressed as a percentage of R6/1 mice and shown as mean ± SEM (n = 3 for R6/1 and n = 4 for R6/1 STEP KO). Data were analyzed by the Student's t-test. *p < .05; **p < .01; ***p < .001; ****p < .0001 compared to R6/1 mice.

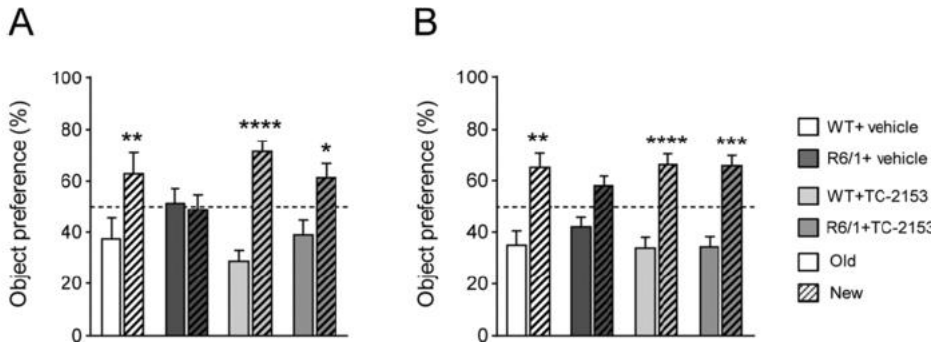

Fig. 4. Pharmacological inhibition of STEP improves cognitive function in R6/1 mice. Vehicle or TC-2153 (10 mg/kg) was administered to 12 week-old WT and R6/1 mice 3 h prior to training sessions of NOLT and NORT. Graphs show the percentage of preference for the object and are expressed as mean ± SEM (n = 5 for WT and R6/1 + vehicle and R6/1 + TC-2153; n = 7 for WT + TC-2153). Data were analyzed by two-way ANOVA with Bonferroni's as a post hoc. *p < .05; **p < .01; ***p < .001; ****p < .0001 compared to old object.